Journal of South American Earth Sciences xxx (2017) 1–13

Contents lists available at ScienceDirect

Journal of South American Earth Sciences

journal homepage: www.elsevier.com/locate/jsames

Geological and geophysical evidences of the polyphase structural evolution of the Southern Precordillera (31°42′S-69°24′W), central-western Argentina

Juan P. Ariza [a, *], Marcos Sánchez [a], Florencia L. Boedo [b], Silvina Nacif [a], Juan P. Contrera [c], Juan P. Ceballos [c], Marcos A. Ludueña [c], Sofía B. Pérez Lujan [b], Graciela I. Vujovich [b], Patricia Martinez [a]

[a] CONICET, Instituto Geofísico Sismológico "Ing. F. Volponi" – UNSJ, Ruta 12 – km 17, Jardín de los Poetas, C.P.5407, Marquesado, San Juan, Argentina
[b] CONICET, Instituto de Estudios Andinos Don Pablo Groeber, Universidad de Buenos Aires, Facultad de Ciencias Exactas y Naturales, Departamento de Ciencias Geológicas, Int. Güiraldes 2160, Pabellón II, 1° Piso, C.P. 1428, Ciudad Universitaria, Ciudad Autónoma de Buenos Aires, Argentina
[c] Departamento de Geología, Universidad Nacional de San Juan, Av. Ignacio de la Roza 590 (O) Complejo Universitario "Islas Malvinas", Rivadavia, San Juan CPA: J5402DCS, Argentina

ARTICLE INFO

Article history:
Received 21 July 2017
Received in revised form
9 November 2017
Accepted 14 November 2017
Available online xxx

Keywords:
Superimposed tectonics
Remote sensing
Aeromagnetic data
Seismic activity

ABSTRACT

The evolution of the western margin of South America comprised different tectonic regimes responsible of the present geological composition and structure of the Central Andes. Remote sensing, geological and geophysical data (aeromagnetic and seismological data) have been processed to understand the polyphase structural evolution of the Argentine Southern Precordillera. The outcrops exposed in the Sierra de Barreal (31°42′S-69°24′W) show evidences of a complex structural evolution related to the superposition of three orogenies from the Early Paleozoic to nowadays. The Chanic orogeny (Late Devonian) is characterized by two systems of non-coaxial ductile folds that affect Early Paleozoic rocks of the Ciénaga del Medio Group. The recognized rotation in the shortening direction (from NW-SE to ENE-WSW) is interpreted here as a result of a sinistral transpressive regime. The San Rafael orogeny (Early Permian) is represented by back-thrusts and blind faults associated to asymmetric folding that involves the deformation of Upper Carboniferous rocks (Majaditas Formation). Finally, the compressive Andean orogeny associated to the Pampean flat-slab subduction segment has been locally controlled by inherited pre-Andean anisotropies. This is evidenced by: 1-the structural style of western-southern Argentine Precordillera, which in the study area is represented by faulted blocks and top-to-west vergent back-thrusts; 2- NW-SE deflections and associated magnetic anomalies in the Argentine Precordillera fold-and-thrust belt; 3-neotectonic structures developed in a sinistral transpressive system; 4-the crustal seismicity associated to NW-SE trending structures with left-lateral component motion.

1. Introduction

The Pacific margin of South America has experienced a long story of orogenic processes which has been preserved in the stratigraphic and structural record of the Andes. The oldest orogenic events are related to the collision of continental blocks (Pampia, Arequipa-Antofalla, Cuyania, among others) against the Gondwana margin between the Neoproterozoic and Middle Paleozoic (Ramos et al., 1986; Dalla Salda et al., 1992; Ramos, 2009; Ramos, 2000; among others). Since Late Paleozoic times the previously consolidated South American margin has been subjected to a generalized subduction process (Ramos, 1999a,b), which has been associated to the development of the San Rafael (Early Permian) and the Andean (Miocene to recent) orogenies. Particularly, during Late Cenozoic times, the Pampean flat-slab subduction segment (27°-33°30′S, Barazangi and Isacks, 1976) favored the generation of landward (dominant east vergent) imbricated thrust sheets (Argentine Frontal Cordillera and Central and Western Precordillera) and the uplift of basement blocks due to the activity of back-thrusts (Argentine Eastern Precordillera and Sierras

* Corresponding author.
E-mail address: jpariza@conicet.gov.ar (J.P. Ariza).

https://doi.org/10.1016/j.jsames.2017.11.012
0895-9811/

Pampeanas) in the front of the Andean orogen (Barazangi and Isacks, 1976; Jordan et al., 1983; Jordan et al., 1993). In this sector, an E-W cross section exhibits different tectonostratigraphic domains corresponding to the previously amalgamated continental blocks and their respective suture zones (Ramos, 1988). These suture zones are coincident with highly deformed and metamorphosed areas with strong positive gravity anomalies (Chernicoff and Zappettini, 2004; Martinez and Gimenez, 2005; Álvarez et al., 2012) that are the key to study the particular features of each orogeny.

This paper is focused on the geology and geophysics of the northern sector of the Southern Argentine Precordillera (Fig. 1), a natural laboratory where three orogenic processes (the Chanic, San Rafael and Andean) are superimposed. Field work, remote sensing and aeromagnetic data were combined in order to understand its polyphase structural evolution. Two different stages were proposed for the evolution of the study area and were integrated in a 3D-model to compare our interpretations with the structural fabric recognized at outcrop scale. Additionally, we present a deep structural model based on the interpretation of focal mechanisms from crustal seismic events that allow us to evaluate the influence of the pre-Andean structures on the active seismicity and recent deformation of the Southern Argentine Precordillera.

2. Geological setting

The Argentine Precordillera is a fold-and-thrust belt located in central-western Argentina, over the Pampean flat-slab subduction segment (Fig. 1a). It has been traditionally divided in an eastern, central and western sector according to their stratigraphic record

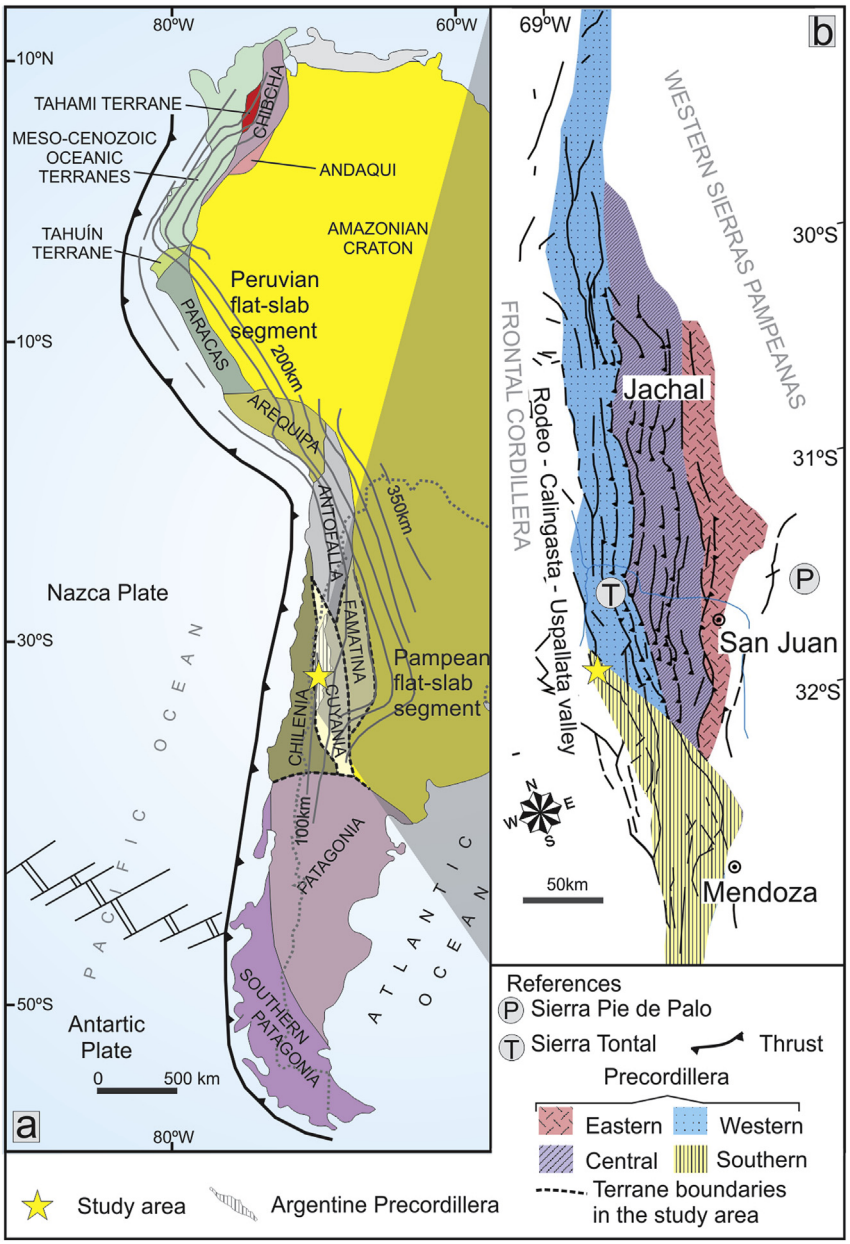

Fig. 1. Location map of study area. a) Location of Precordillera Argentina in the context of South American terranes docked to the western margin of Gondwana (modified from Ramos, 2009). Continuous grey lines represent the top of the subducted Nazca plate. b) Subdivision of Precordillera on the basis of its stratigraphic and structural features (from Baldis and Chebli, 1969; Ortiz and Zambrano, 1981; Baldis et al., 1982; Cortés et al., 2005).

Please cite this article in press as: Ariza, J.P., et al., Geological and geophysical evidences of the polyphase structural evolution of the Southern Precordillera (31°42′S-69°24′W), central-western Argentina, Journal of South American Earth Sciences (2017), https://doi.org/10.1016/j.jsames.2017.11.012

and structural features (Fig. 1b, Baldis and Chebli, 1969; Ortiz and Zambrano, 1981; Baldis et al., 1982). Recently, Cortés et al. (2005, 2006) defined the Southern Precordillera (Fig. 1b), a second order morphotectonic unit located south of 31°30′S that consists of 20–30 km long NNW- to NNE-trending blocks and irregular quaternary basins. It is also characterized by longitudinal inverted normal faults associated to thrusts and to NW-NNW oblique sinistral faults.

The study area is located in the northernmost sector of the Southern Argentine Precordillera and includes the southern sector of the Sierra de Barreal (Fig. 1b). The early Paleozoic stratigraphy has been defined and reviewed by several authors (Amos and Marchese, 1965; Quartino et al., 1971; Gaido et al., 2008; among others).

2.1. Local stratigraphy

2.1.1. Ciénaga del Medio Group (Devonian?)

This group was defined by Amos and Marchese (1965) and it is composed from bottom to top by three lithostratigraphic units developed in a marine environment: the Hilario Formation (HF), the Lomitas Negras Formation (LNF) and the Tontal Formation (TF). HF is composed by medium-grained metagreywackes and feldespathic metasandstones with subordinated shales. Chondrites trace fossils are present (Furque and Cuerda, 1979). It is conformably covered by green and purple shales of the Lomitas Negras Formation. The Tontal Formation is represented by massive greenish-grey metasandstones and a few greenish-grey shales.

The thickness of the group is unknown due to its intense deformation. In the study area, it is unconformably covered by Upper Carboniferous rocks (Majaditas Formation, Fig. 2a). It is assigned to the Lower-Middle Devonian on the basis of stratigraphic correlations and fossiliferous content (Baldis, 1975; Baldis and Peralta, 1999 and references therein). To the south, in the Cordón Sandalio and Cerro Redondo areas, Cortés (1992) assigned it to the Silurian-Devonian due to findings of plant remnants.

Basaltic dikes and sills intrude the sandstones of the Tontal Formation (Fig. 2b). They exhibit porphyritic texture with plagioclase and amphibole phenocrysts within a groundmass of trachytic texture. This igneous assemblage is partially replaced by an association of chlorite, carbonates, quartz and opaque minerals. Quartz crystals show evidences of internal deformation with the development of sub-grains with irregular borders.

A penetrative foliation associated to a low-grade metamorphic event affects both the metabasalts and the metasedimentary rocks of the Ciénaga del Medio Group (Fig. 2b).

2.1.2. Majaditas Formation (Upper Carboniferous)

This unit was also defined by Amos and Marchese (1965) who attributed it to a glacial marine environment. In a detailed study, Lopez Gamundí (2001) recognized a fining-upward sequence where the base consists of clast-supported conglomerates and subordinate coarse-to medium-grained sandstones, pebbly mudstones and diamictites. In the study area, the conglomerates uncomformably lie over the rocks of the Ciénaga del Medio Group. Towards the top the unit consists of thin-bedded, low-density turbidites; well sorted, coarse-to medium-grained sandstones and subordinate bioturbated and laminated mudstones.

In the study area, this unit is intruded by dacitic dikes and sills of up to 3 m thick belonging to Cerro Redondo Formation (Cortés, 1992). Leveratto (1976) assigned them to the Miocene, whereas to the south, in the Cortaderas and Bonilla areas, Davis et al. (1999) dated similar rock bodies in 11.2 ± 0.1 Ma (Ar-Ar in biotite) and 17.6 ± 0.3 Ma (Ar-Ar in hornblende).

2.1.3. Lomas del Inca Formation (Paleogene-Neogene)

This unit was defined by Baldis (1964) and crops out in the northern part of the Sierra de Barreal area. It consists on coarse-grained silicoclastic deposits which progressively passes to the south to fine-grained deposits. Yamín (2007) recognized a lower member consisting on conglomerates and coarse-grained sandstones, a middle member of conglomerates, sandstones and tuffs and an upper member composed by sandstones, conglomerates and tuffs. Conglomerates and tuffs of the middle member uncomformably cover the beds of the Majaditas Formation.

2.1.4. Piedmont deposits (lower-middle Pleistocene)

This unit corresponds to ancient piedmont deposits that consists on coarsening-upward sequences. Yamín (2007) recognized two levels of piedmont deposits of lower-middle Pleistocene age: the lower level is represented by conglomerates and sandstones with a source area located in the Precordillera, while the upper level is characterized by conglomerates and sandstones whose source area is the Frontal Cordillera.

2.2. Structure of the southern Sierra de Barreal

2.2.1. Ductile folds

These folds affect the Early Paleozoic rocks and are divided into two systems according to the scale of folding. In the study area, the first system is represented by NNE-SSW-trending folds, minor folds and axial plains (Fig. 2c–d). These folds have wavelengths of tens meters and are represented by alternating anticlines and synclines. The second system has wavelengths that range from tens to hundreds of meters (Fig. 2c). These folds are visible in satellite imagery scale by the application of remote sensing data.

2.2.2. Minor structures associated to folding

At an outcrop scale, minor folds with centimetre wavelength associated with pencil structures are recognized. The latter structure results from the intersection between the foliation parallel to the bedding (S_0) and the axial-plane cleavage (S_1) which is represented by fractures (Fig. 2b). A conspicuous brightness is associated to the foliation parallel to the bedding.

2.2.3. Faulting and associated folds

The Carboniferous rocks are affected by NNE-SSW asymmetric syncline-anticline folds with axes between 200°/51° and 183°/67° (Fig. 2e). Moreover, as shown below, these folds are spatially related with a main NNW-SSE structural lineament on the central part of the Sierra de Barreal.

The Andean fold-and-thrust belt has general eastward vergence. However, along the Southern and Western Precordillera there are systems of back-thrusts where Miocene rocks are overthrusted by Paleozoic rocks (Giambiagi et al., 2010, 2014; Ariza et al., 2015; among others). Well documented neotectonic structures present on the western piedmont of the Southern Precordillera (Cortés et al., 2005; Yamín, 2009) indicate that the mentioned back-thrusts are still active.

3. Data, methods and results

3.1. Remote sensing

Landsat 7 ETM satellite data employed was acquired through the Global Land Cover Facility website (http://glcf.umiacs.umd.edu) which belongs to the University of Maryland and National Aeronautics and Spatial Administration (NASA). The acquisition date of the selected image (path: 232, row: 082) corresponds to 3 December 1999. The images employed have high spatial resolution,

Please cite this article in press as: Ariza, J.P., et al., Geological and geophysical evidences of the polyphase structural evolution of the Southern Precordillera (31°42′S-69°24′W), central-western Argentina, Journal of South American Earth Sciences (2017), https://doi.org/10.1016/j.jsames.2017.11.012

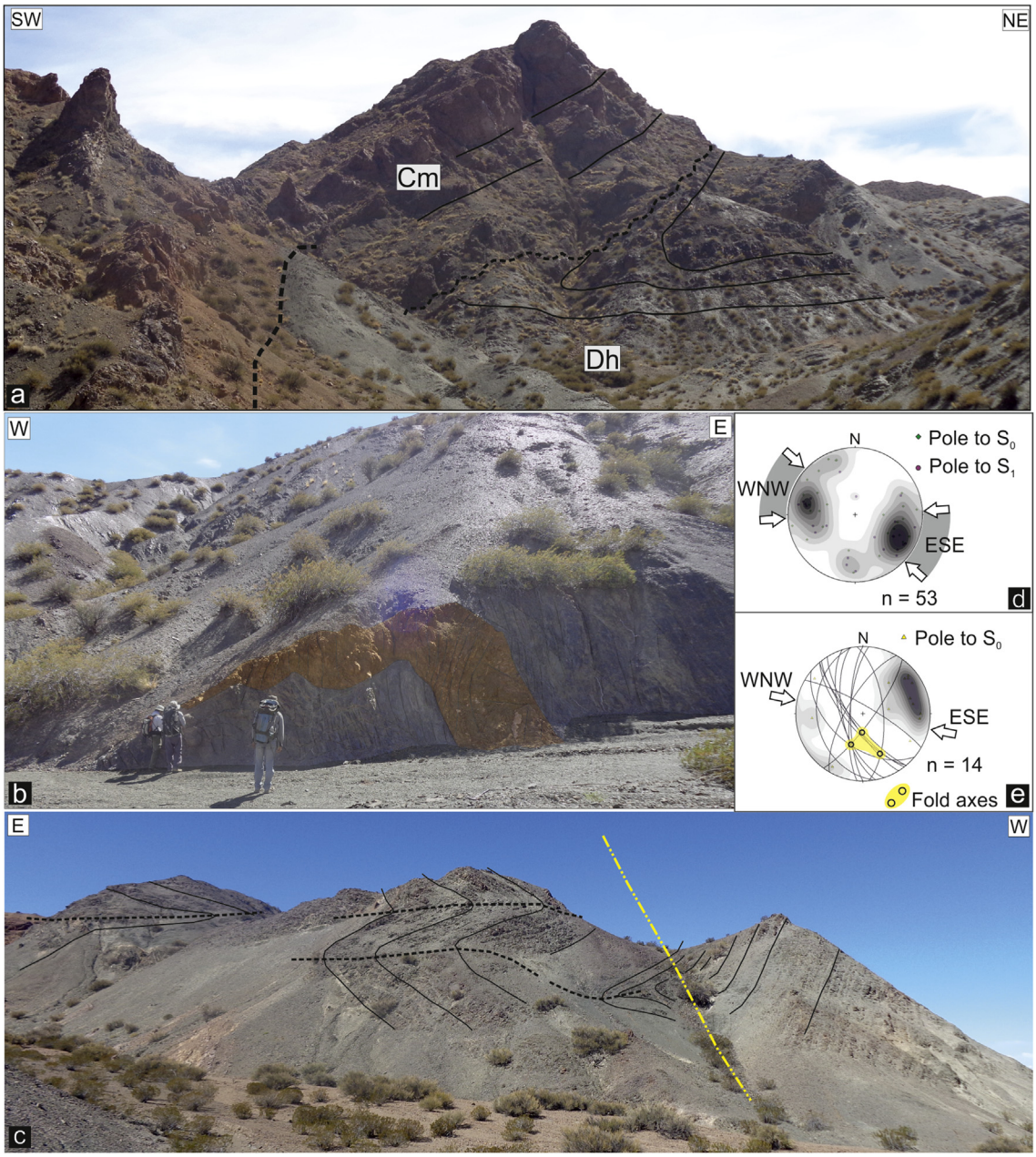

Fig. 2. Pre-Andean structures. a) Folded beds of Hilario Formation (grey) and basaltic dike/sill (orange). The dashed lines represent the primary layering (S_0) while the continuous lines indicate the axial plane cleavage (S_1). Note the refraction of the cleavage when it crosses layers of different composition. b) Interference of folds. The two systems of Chanic folds along a E-W cross-section. The continuous lines correspond to primary layering (S_0) while the discontinuous black lines indicate the axial planes of the first folding system; the dashed yellow line indicates the refolding planes. c) Angular unconformity between the Majaditas Formation (Cm, Upper Carboniferous) and Hilario Formation (Dh, Devonian). d) – e) Lower hemisphere, equal area stereoplots of the structural data corresponding to: d) (Chanic structures) S_0 primary layering and S_1 axial plane cleavage. The white arrows indicate the direction of main shortening while the shaded area between them indicates the rotation from NW-SE to ENE-WSW of the main associated efforts **e)** (San Rafael structures) great-circle representation of Upper Carboniferous beds. The little circles correspond to the fold axis. (For interpretation of the references to colour in this figure legend, the reader is referred to the web version of this article.)

high spectral range, radiometric calibration and provide information in the near infrared and visible channels (NIR), short wave infrared (SWIR), thermal infrared (TIR) and panchromatic. The image wide size is 183 km and its spatial resolution is 28.5 m in bands 1 to 5 and 7; 15 m in band 8; and 60 m in band 6.

Different techniques of satellite imagery processing were applied through the software ENVI 4.5, such as combination of bands, spectral classifications (supervised and unsupervised) and band ratios (Lillesand and Kiefer, 1994; Inzana et al., 2003; Gad and Kusky, 2006; among others). The latter technique provided the best results to separate lithostratigraphic units (Fig. 3) and to clarify the structural setting.

3.1.1. Band ratios

We applied the band ratios 7/5, 5/4, 3/1 (Fig. 3) since they are suitable for discrimination between granites, mafic, sedimentary and metavolcanic rocks (Gad and Kusky, 2006).

The results obtained by remote sensing techniques (Table 1) allowed us to recognize boundaries between the different lithostratigraphic units and their spatial distribution (Fig. 3). Each unit

Please cite this article in press as: Ariza, J.P., et al., Geological and geophysical evidences of the polyphase structural evolution of the Southern Precordillera (31°42′S-69°24′W), central-western Argentina, Journal of South American Earth Sciences (2017), https://doi.org/10.1016/j.jsames.2017.11.012

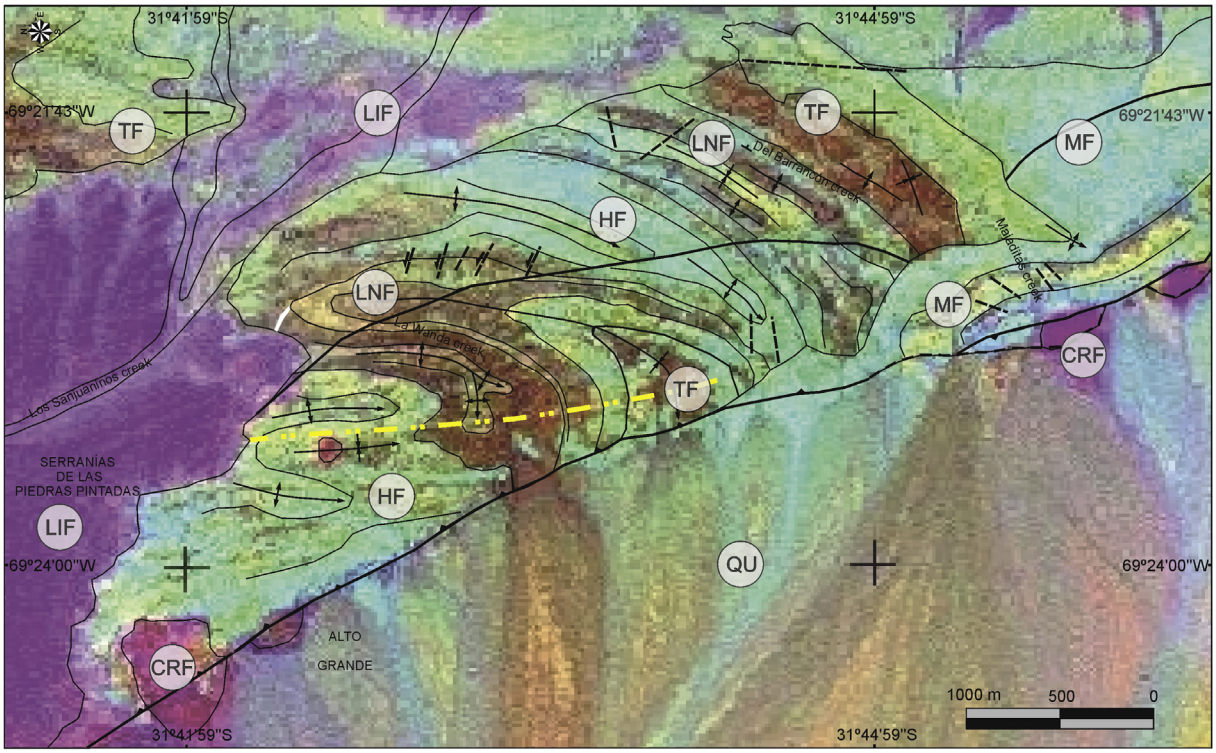

Fig. 3. Processed LANDSAT7 satellite image. Distribution of the lithostratigraphic units on a false color image processed by band ratios R7/5 G5/4 B3/1. HF: Hilario Formation, LNF: Lomitas Negras Formation, TF: Tontal Formation, MF: Majaditas Formation, LIF: Lomas del Inca Formation, QU: Quaternary Piedmont deposits. The fine black lines represent lithological breaks while the thick black lines correspond to the trace of the backthrusts (see detailed structural references on the geological map, Fig. 5). (For interpretation of the references to colour in this figure legend, the reader is referred to the web version of this article.)

has one or more well defined colors (Table 1) which together contribute to outline its contacts. The shape of these contacts and their distribution allowed us to build the geometry of the secondary structures which were acquired by tectonic deformation (folding and faulting).

3.2. Magnetism

In order to characterize and recognize geological structures, different filters have been applied to the high resolution magnetic database. This was obtained from the Servicio Geológico Minero Argentino, (SEGEMAR) and corresponds to Zone 17-Block II Precordillera Sur (Mendoza-San Juan). Measurements were collected by the acquisition company Sial Geosciences, at a nominal height of 120 m along N-S flight lines spaced every 1000 m and E-W flight control lines every 7500 m. Thirty seven control lines were used along the original magnetic coverage. This database was then corrected for the daily variation by the aforementioned company (Dobrin, 1976). Magnetic anomaly was calculated by subtracting from dataset the International Geomagnetic Reference Field (IGRF) at the acquisition date (Blakely, 1996). The levelling of the aerial magnetic data was performed following the methodology proposed by Cheesman et al. (1998) and Ruiz et al. (2011). This was carried out using terrestrial magnetic data which improves the resolution from a 5 × 5 km to a 250 × 250 m cell size.

The obtained magnetic anomaly map is shown in Fig. 4a. The relation between the magnetic anomaly and the paleozoic rocks is not so clear. It is noteworthy that the maximum values at −23 nT are reached towards the NW direction where the outcrops of the dacitic rocks are located.

3.2.1. Filtering of anomalies-upward continuation

Analytical continuation of potential fields has been widely used as a filter in frequency domain. Specifically, upward continuation allows to evaluate the potential field measured on a surface ($h = 0$, usually the topography or flight-elevation), over another plane which attenuate high-wavenumbers ($h \neq 0$) from bodies emplaced on the upper crust (Dean, 1958; Blakely, 1996).

Upward continuations at different heights were calculated. An optimum surface $h = 6.5$ km was selected as a regional magnetic

Table 1
Results obtained by band ratios applied to satellite imagery.

Geologic unit	Age	Lithology	Remote sensing Technique	Range of colors
Piedmont deposits	Quaternary	Sandstones and conglomerates	Band ratios R7/5 G5/4 B3/1	Brown pinkish
Lomas del Inca Fm.	Paleogene-Neogene	Conglomerates, sandstones and tuffs		Purple
Cerro Redondo Fm.	Neogene	Dacite		Purple
Majaditas Fm.	Upper Carboniferous	Conglomerates, sandstones and pelites		Light blue, green and with
Tontal Fm.	Devonian	Sandstones and pelites		Brown redish and light green
Lomitas Negras Fm.	Devonian	Shales		Brown and green yellowish
Hilario Fm.	Devonian	Coarse sandstones		Light blue and green yellowish

Please cite this article in press as: Ariza, J.P., et al., Geological and geophysical evidences of the polyphase structural evolution of the Southern Precordillera (31°42′S-69°24′W), central-western Argentina, Journal of South American Earth Sciences (2017), https://doi.org/10.1016/j.jsames.2017.11.012

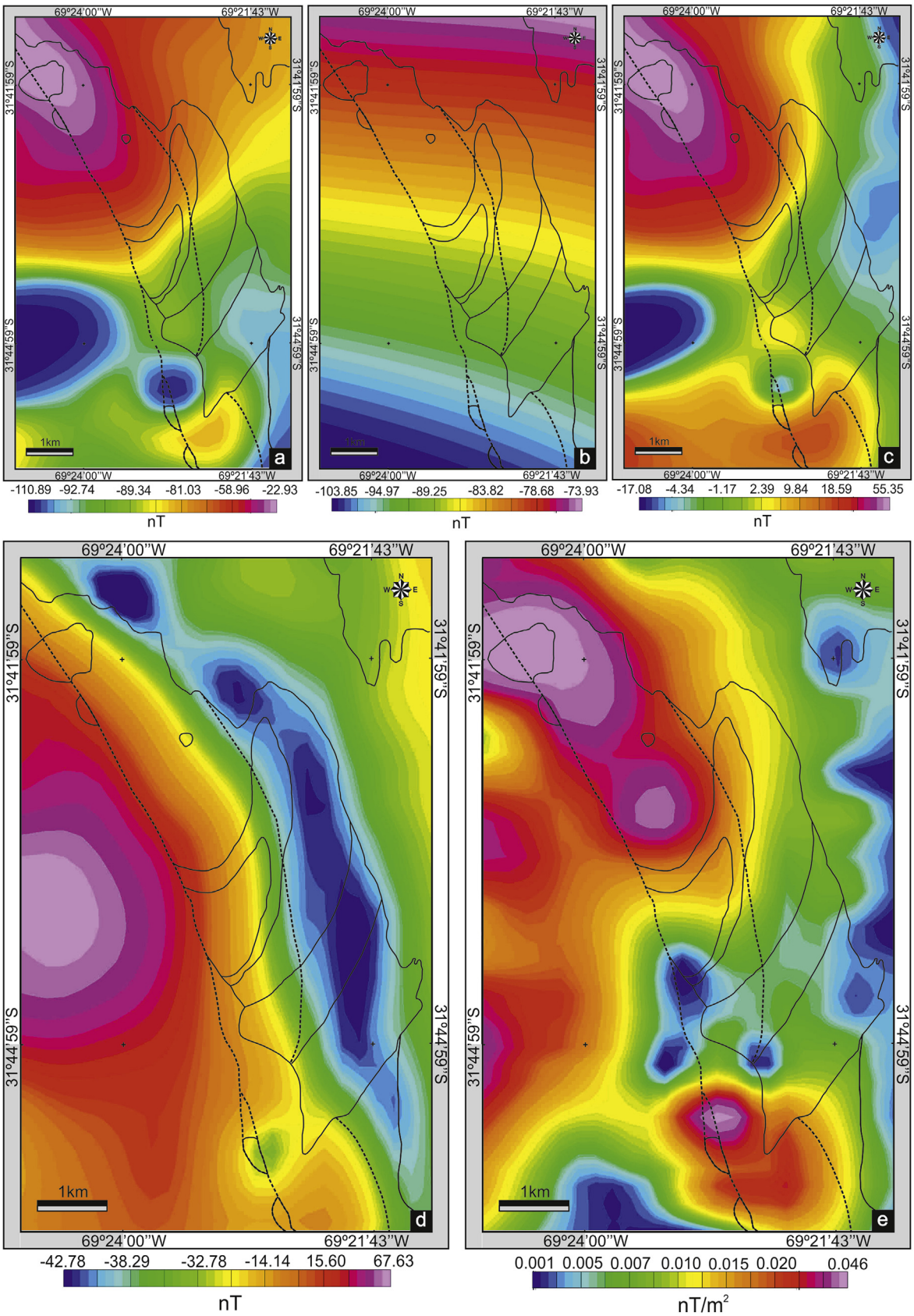

Fig. 4. Magnetic maps of the Sierra de Barreal (the black continuous lines correspond to lithological breaks and dashes lines indicate the trace of the main backthrusts. a) Observed Magnetic Anomaly Field. b) Regional Magnetic Anomaly Field corresponding to the upward continuation on a reference plane located at 6.5 km c) Residual Magnetic Anomaly Field resulting from the removal of the regional effects present in the observed-magnetic anomaly. d) Reduce to magnetic pole. e) Analytical signal map.

Please cite this article in press as: Ariza, J.P., et al., Geological and geophysical evidences of the polyphase structural evolution of the Southern Precordillera (31°42′S-69°24′W), central-western Argentina, Journal of South American Earth Sciences (2017), https://doi.org/10.1016/j.jsames.2017.11.012

anomaly field (Fig. 4b) showing a general decreasing trend south-westwards. The residual magnetic anomaly field (Fig. 4c) was obtained by subtracting the regional anomaly to the magnetic anomaly.

3.2.2. Reduction to magnetic pole

Reduction to pole (RTP) is a method applied to magnetic data that removes the asymmetry caused by the non-vertical direction of magnetization (Baranov, 1975; Phillips et al., 2007).

The RTP method takes the total-observed magnetic field transforming it and producing a map that would have resulted considering the area in the terrestrial magnetic pole (magnetic inclination = 90°). Such transformation produces a displacement of the recalculated magnetic anomaly which places over the anomalous source. This technique allowed us to adjust the longitudinal extension of a structural lineament in the central part of the Sierra de Barreal where its northward and southward continuity is not clearly visible. The obtained RTP map (Fig. 4d) shows a significant magnetic contact which is developed along the central part of the Sierra de Barreal. This magnetic contact matches with a main fault trace which has a NNW-SSE trend at the central part of the Sierra de Barreal and a NW-SE trend to the north and south.

3.2.3. Analytical signal

This method is used to enhance the high frequency anomalies through the calculation of the horizontal and vertical derivate of the magnetic anomalies (Nabighian, 1972, 1984; Roest et al., 1992). High frequency anomalies are frequently associated to magnetic contrasts related to lithological, tectonic contacts or the distribution of the dacite bodies. Moreover, the NW-SE trend of the maximum analytical signal values is laterally bounded by the equally oriented main thrusts and pre-Andean folds.

3.3. Geological map of the Sierra de Barreal

The aforementioned data and results are combined in the geologic map of the Sierra de Barreal (Fig. 5). The Ciénaga del Medio Group are the most representative outcrops in the study area. It is tectonically repeated since it is involved in the main structure of the mountain, which is represented by different scale anticline-syncline ductile folds.

The Majaditas Formation occupy the core of a syncline on the south-eastern sector of the Sierra de Barreal (Fig. 5), where the steep beds of the eastern flank mark the beginning of an asymmetric anticline to the east. The Ciénaga del Medio Group rocks crop out in the core of this anticline. Sedimentary rocks of Lomas del Inca Formation mainly crop out to the northeast of the Sierra de Barreal where they are part of low intermontane areas. The dacite bodies (Cerro Redondo Formation) form discontinuous outcrops closely related to the back-thrusts on the western flank of the Sierra de Barreal. The piedmont deposits cover important areas on the south-western sector of the study area.

3.4. 3D-model

We performed a 3D-model employing the software “Visible Geology” (http://visible-geology.appspot.com). It is based on our interpretation about how the structures evolved through time. Since our structural model includes a polyphase evolution, we separated the structural evolution in two stages (“early” and “late”) that correspond to the main sedimentary and orogenic events recognized in the study area.

The early stage includes the geological events developed during Early Paleozoic times: 1- The sedimentation of the Ciénaga del Medio Group (Fig. 6a); 2- The development of the Chanic orogeny which is represented by overlapped non-coaxial folds and a westward vergent back-thrust (Fig. 6b–g).

The late stage includes the geological events developed between Late Paleozoic and Cenozoic times: 1- The onlap of the Majaditas Formation over the previously deformed Ciénaga del Medio Group (Fig. 7a); 2- The development of faulting (blind thrust) and associated folds that corresponds to the San Rafael orogeny (Fig. 7b–c); 3- The onlap of neogene deposits over the pre-Andean rocks to the east (Fig. 7d) and active back-thrusts on the western flank of the Sierra de Barreal (Barreal fault, Fig. 7e). An extensional stage is regionally recorded for the Triassic. However, our model does not include it due to unclear structural evidences and the absence of stratigraphic record in the study area. Moreover, a high-angle fault in the central part of the range would be the result of an Andean reactivation along the previous blind fault. Although its participation during the extensional triassic event is not ruled out. Both fault systems affect paleozoic and miocene rocks in the study area.

3.5. Deep and shallow sources of local seismicity

The facilities of the IRIS Data Management System were used for access to waveform required in this study. Particularly, we employed the seismological data provided by CHile ARgentina Geophysical Experiment (CHARGE) recorded from November 2000 to May 2002. In this experiment the stations were set in two east-west cross sections at approximately 30°S and 36°S, with other stations located between them (Fig. 8). Fig. 8 shows the seismic events that occurred in the study area and its surroundings reported by the National Earthquake International Centre of the United States Geological Survey (NEIC-USGS). Considering that in this region the majority of earthquakes have magnitudes less than 5, only one focal mechanism solution (Mw 5.3, March 11, 2009) in a period of 35 years is available from the Global Centroid Moment Tensor Catalog (GCMT). Recently, Ammirati et al. (2015) presented the relocation of that GCMT solution together with other focal mechanism solutions obtained by waveform inversion. Some of those solutions are compared here with our results (Fig. 8).

In the study area, the only earthquake reported by the NEIC Catalog is the event of local magnitude 3.1 occurred on March 20, 2002 (white and yellow fault plane solution symbol “beach ball” in Fig. 9). From the continuous register by the CHARGE network, we selected the waveform in which this earthquake occurred. We located the earthquake using Hypocenter (Liener and Havskov, 1995) with the 1D velocity model published by Furlani (2015). The final result is located at ~15 km to the northwest and 11 km deeper compared to the NEIC reported location (Table 2) whose graphical uncertainties is represented by an ellipse of error. Focal mechanism solution was derived from P first motion polarities using HASH code (Hardebeck and Shearer, 2002) in SEISAN platform (Havskov and Ottemoller, 2010). A total of 25 phases were picked (13 P and 12 S) coming from 11 stations (Figs. 9 and 10). A strike-slip solution was found (Table 3) and its strike uncertainties are shown in Fig. 10. The first nodal plane (72.9°; 78.2°SE) has dextral strike slip, while the second one (342.8°; 87.6°NE) has sinistral strike slip (Fig. 9).

3.5.1. Structural model

A general structural model along a cross-section A-B is shown (see location on Fig. 8). The geological and seismological features were incorporated from previous works of Ramos et al. (2002) and Ammirati et al. (2015). However, some modifications to the structural setting of Southern Precordillera (Fig. 11) have been made from the interpretation of our data and the reinterpretation of three solutions of Ammirati et al. (2015). In this context, the structure of Southern Precordillera is characterized by a double-vergence

Please cite this article in press as: Ariza, J.P., et al., Geological and geophysical evidences of the polyphase structural evolution of the Southern Precordillera (31°42′S-69°24′W), central-western Argentina, Journal of South American Earth Sciences (2017), https://doi.org/10.1016/j.jsames.2017.11.012

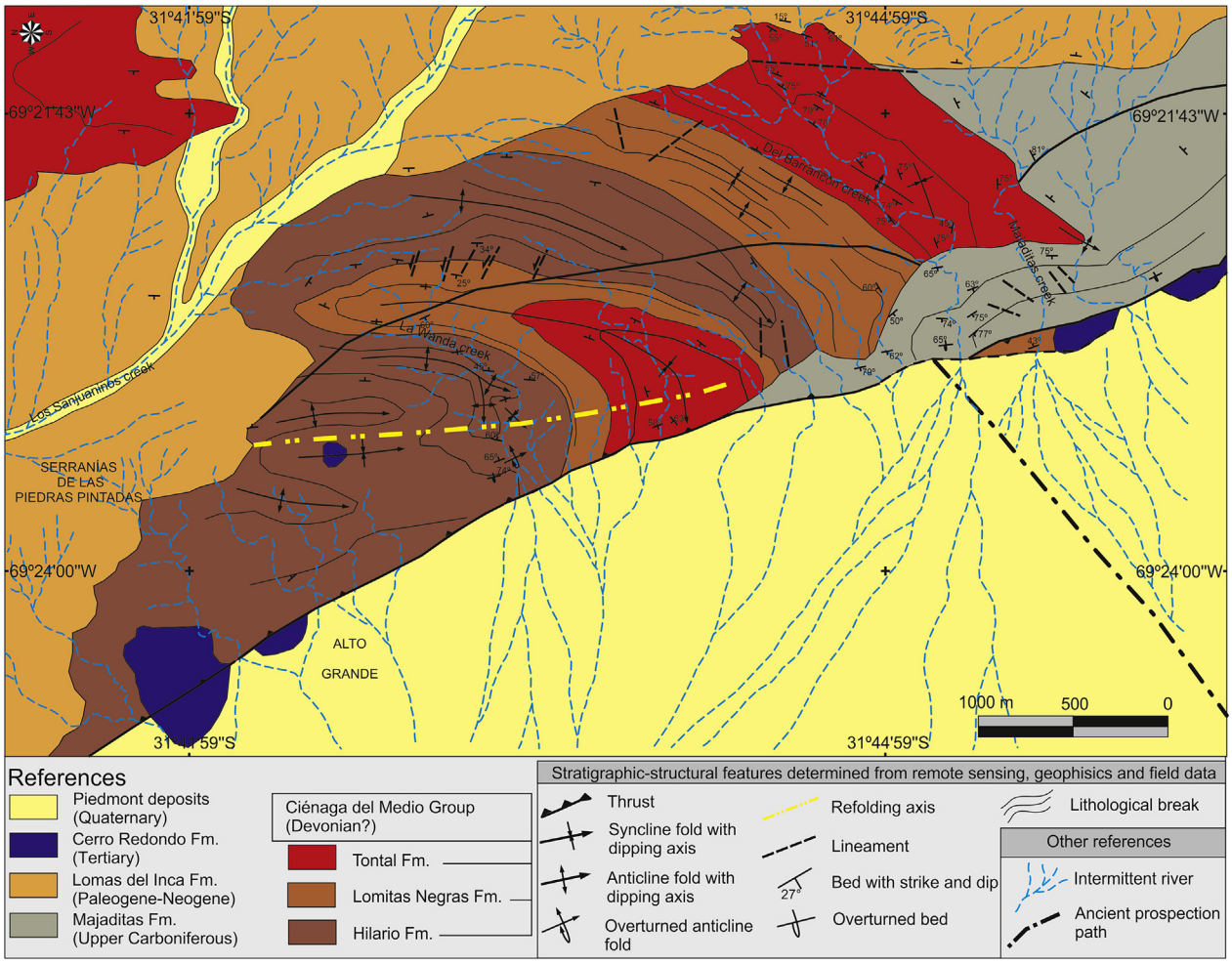

Fig. 5. Geological map of the southern Sierra de Barreal (modified from Quartino et al., 1971; Gaido et al., 2008).

system of thrusts (Baldis et al., 1982; Cortés et al., 2005; among others). Particularly, the close location of the studied earthquakes in relation to those top-to-west vergent back-thrusts seems to indicate their control on the active seismicity at different crustal levels (Fig. 11). This relation was used to discard the top-to-east nodal plane on the focal mechanisms proposed by Ammirati et al. (2015). The second nodal plane obtained in this work (342°; 87°NE, Table 2) would be the most plausible solution because it has a dominant NNW-SSE trend and a left-lateral component motion as those neotectonic structures documented by Gaido et al. (2008) to the southeast of the Sierra de Barreal.

4. Interpretation and discussion

The western margin of the Argentine Precordillera exhibits a complex geological evolution that includes: the opening of an Early Paleozoic extensional basin and its closure during the late Devonian (Chanic orogeny); the development of the San Rafael orogeny during early Permian times; the extensional regime occurred during the Triassic and the Andean orogeny since the Miocene. The Southern Precordillera is a natural laboratory where a better understanding of how pre-Andean structures have controlled recent geological processes can be achieved.

The Chanic orogeny is the oldest tectonic event recognized in the study area. In the field, this orogeny is represented by two systems of ductile folds which are associated to greenschist facies metamorphism (Robinson et al., 2005; Davis et al., 1999; Willner et al., 2011; Boedo et al., 2016). Such structures belong to the pre-Carboniferous evolution of the area as documented by the regional unconformity between early paleozoic rocks and carboniferous deposits (Amos and Rolleri, 1965; Ramos et al., 1986) and the K/Ar on whole-rock, Ar/Ar on white mica and Lu-Hf on garnet ages (~390 Ma, Cucchi, 1971; Buggisch et al., 1994; Davis et al., 1999; Willner et al., 2011). Although there is a general consensus that the Chanic orogeny represents the collision between the Chilenia and Cuyania terranes (Ramos et al., 1986; Astini, 1992; Davis et al., 1999; among others), different models have been proposed for the processes involved during the closure of the Early Paleozoic marine basin and the final amalgamation of the aforementioned terranes (Ramos et al., 1986; Davis et al., 2000; Willner et al., 2011; Heredia et al., 2012; Giambiagi et al., 2014; Ariza, 2016; among others).

All the models proposed involve strong compression. Giambiagi et al. (2010) proposed that the occurrence of two directions of folding could be the result of two different orogenic events or the rotation of the shortening direction during the same event. In a similar way, the two systems of non-coaxial folds recognized in this work can be interpreted as the result of the continuous folding of the Early Paleozoic rocks where the rotation of the shortening direction (from NW-SE to WSW-ENE) would better explain a sinistral transpressive system than a pure compressive system.

Structures related to the Chanic orogeny probably controlled the Late Paleozoic deformation (von Wosen, 1995; Giambiagi et al.,

Please cite this article in press as: Ariza, J.P., et al., Geological and geophysical evidences of the polyphase structural evolution of the Southern Precordillera (31°42′S-69°24′W), central-western Argentina, Journal of South American Earth Sciences (2017), https://doi.org/10.1016/j.jsames.2017.11.012

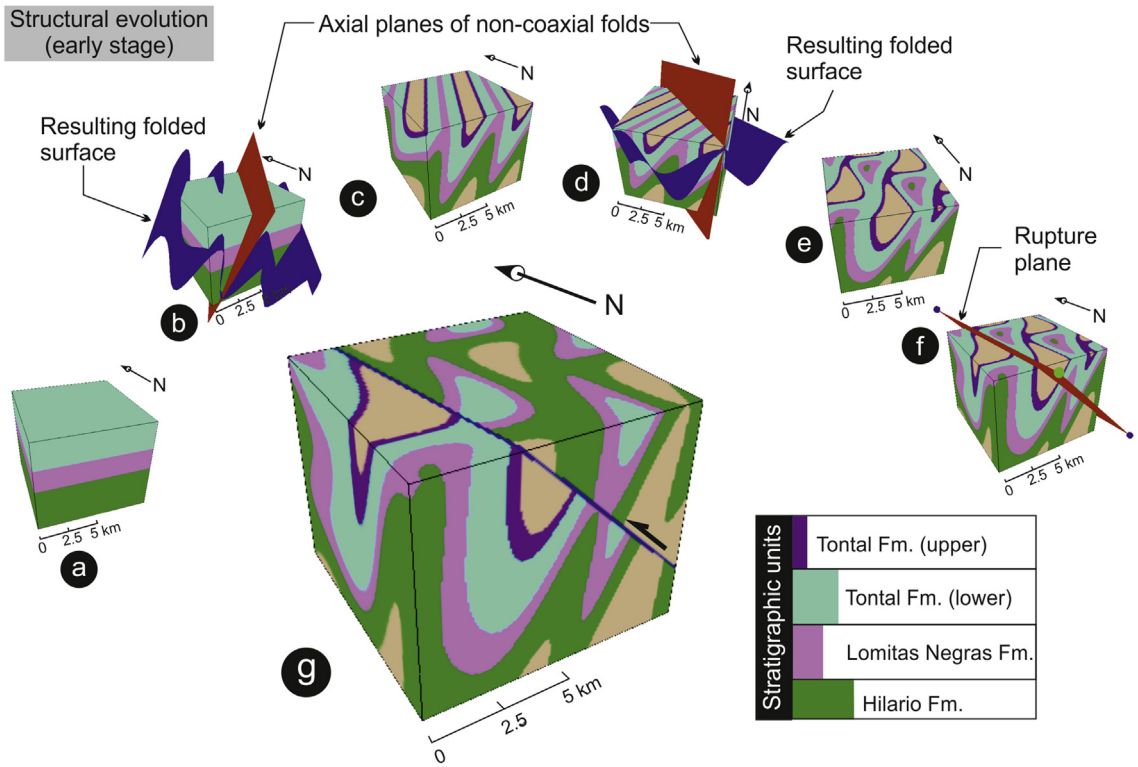

Fig. 6. 3D models of pre-Carboniferous structural evolution. a) Continuous sedimentation stage of the Ciénaga del Medio Group during Early Devonian. b)-e) Overposition of non-coaxial Chanic folds (Late Devonian). b)-c) Development of the first system of folds along a NE-SW-trend. d)-e) Refolding stages along a NW-SE-trend. e) Interference pattern of folds. f) Inception of an inferred backthrusts on the western margin of the Sierra de Barreal. g) Resultant outcrops design obtained by the superposition of each stage of the structural evolution.

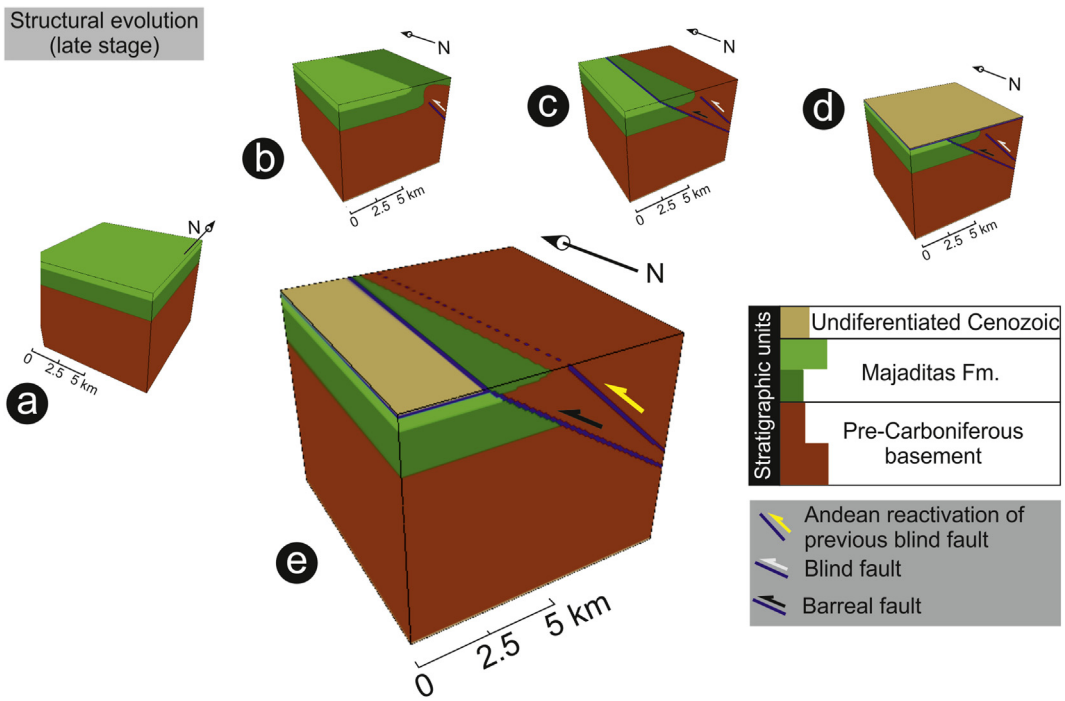

Fig. 7. 3D models of the structural evolution between Early Permian and Neogene. a) Sedimentation stage of Upper Carboniferous deposits (Majaditas Formation) on the previously deformed units (pre-Carboniferous basement). b) – c) Blind faulting and associated folds during San Rafael orogeny (Early Permian) by reactivation of previous backthrusts. d) Unconformably sedimentation of Neogene deposits (Lomas del Inca Formation) on pre-Andean units. e) Resultant outcrops design obtained by the superposition of each stage of the structural evolution. This stage includes the reactivation of the backthrusts from the Miocene to nowadays.

Please cite this article in press as: Ariza, J.P., et al., Geological and geophysical evidences of the polyphase structural evolution of the Southern Precordillera (31°42′S-69°24′W), central-western Argentina, Journal of South American Earth Sciences (2017), https://doi.org/10.1016/j.jsames.2017.11.012

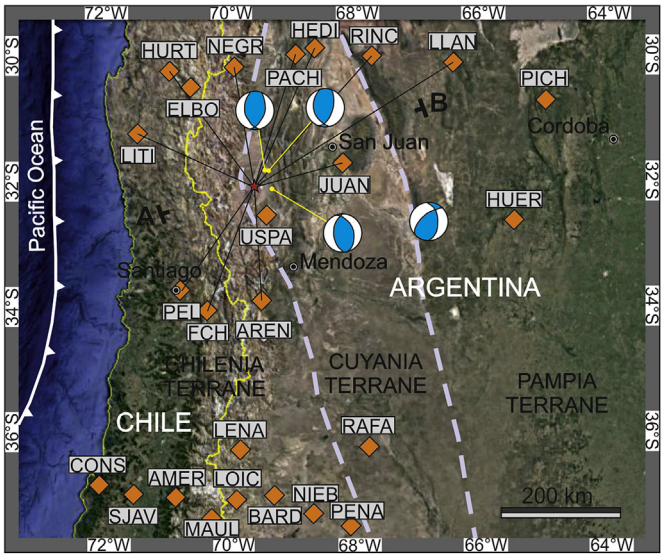

Fig. 8. Seismological stations (orange diamond) from CHARGE network except PEL station which belongs to the global seismological network (GEOSCOPE). The red star represents the earthquake processed in this study and the black lines point out the used stations. Focal mechanisms (light blue and white beach balls) from Ammirati et al. (2015) are shown. A–B: location of the cross-section represented in the structural model. (For interpretation of the references to colour in this figure legend, the reader is referred to the web version of this article.)

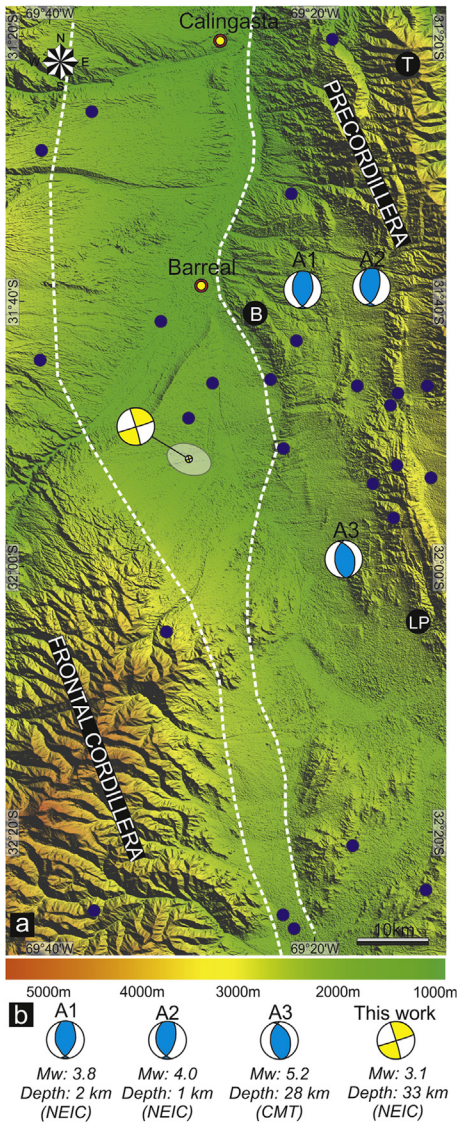

Fig. 9. Epicenters at the study region and surrounding areas (blue points) from NEIC Catalog (1977–2012). The white and yellow beach ball represent the focal mechanism associated to the earthquake processed in this study. Mechanisms from Ammirati et al. (2015) are shown (light blue and white beach balls). The grey ellipse represents graphically the error in the location of the studied earthquake. B – LP: Barreal – Las Peñas belt. The white dashed lines represent the limits between Frontal Cordillera and Precordillera. (For interpretation of the references to colour in this figure legend, the reader is referred to the web version of this article.)

2014; this work). In the study area, the morphology of the syncline-anticline folds developed in the Majaditas Formation on the southwest of the Sierra de Barreal (Fig. 7b) is interpreted here as folds associated to a blind reverse fault which was probably generated along an inherited chanic structural anisotropy. In the northern part of the Sierra de Barreal, the upper Carboniferous folded beds are unconformably covered by undifferentiated triassic pyroclastic rocks (Mesigos, 1953). Such unconformity has been regionally interpreted as an evidence of the San Rafael orogeny (Azcuy and Caminos, 1987; Ramos, 1988) which generated a wide NW to NNW-trending orogenic belt with important crustal thickening on the western active margin of Gondwana during the early Permian (Llambías and Sato, 1990; Mpodozis and Kay, 1990; Giambiagi et al., 2012).

The design of the magnetic anomalies obtained in this work reflects the current surface distribution of geological units and structures. Thus, the regional magnetic anomaly shows the influence of deep regional sources on the total magnetic anomaly field. Therefore, in a regional magnetic anomaly map is common to find along the Andean orogen a west-dipping potential field surface corresponding to a deepening of the Andean roots. As in other localities of the Precordillera (Ariza et al., 2015), our regional magnetic anomaly map shows a decreasing magnetic anomaly trend south-westwards (Fig. 4b). These local defections of the magnetic anomaly field would be produced by NW-SE deep structures or ancient lineaments located in the basement of the Precordillera (Japas, 1998; Ré et al., 2001; Ariza et al., 2015). Regarding the neogene magmatic rocks, the NW-SE elongated design and the distribution of the residual magnetic anomaly (Fig. 4c) seem to indicate that both the emplacement of the dacitic bodies and its magnetical signature were controlled by the pre-Andean structures. Besides, the maximum values of the analytical signal bounded by the two main back-thrusts of the Sierra de Barreal (Fig. 4e) support this interpretation.

The current seismicity at this latitude can be separated in two groups: a slab seismicity deeper than 90 km and a crustal seismicity mainly less than 40 km deep (Ammirati et al., 2015). The seismicity under the Sierra de Barreal interpreted here is within the second group. The alignment of the seismicity under the Sierra de Barreal adjusts better with westward vergent back-thrusts. However, this design would be associated to a main detachment located in the basement (28 km deep). This coincides with the CMT reverse focal mechanism studied by Ammirati et al. (2015). Within the context of our proposed structural model, we reinterpret the two shallow focal mechanisms determined by Ammirati et al. (2015) as seismic events related to the back-thrusts of the Western and Southern Precordillera. The left-lateral component motion of the focal mechanism determined in this paper would be the result of NW-SE-trending regional structures oblique to the Andean convergence N76°E (DeMets et al., 1990). Recently, Rivas (2017) proposed a compressive tectonic setting (σ1: 100°/16° - σ2: 194°/12° - σ3:

Please cite this article in press as: Ariza, J.P., et al., Geological and geophysical evidences of the polyphase structural evolution of the Southern Precordillera (31°42′S-69°24′W), central-western Argentina, Journal of South American Earth Sciences (2017), https://doi.org/10.1016/j.jsames.2017.11.012

Table 2
Location parameters of the studied seismic event.

Seismic Event Parameter					
Origin Time	Location Parameters			Location Uncertainties	
Year/Month/Day/Hour/Min./Sec	Lat. (°)	Long. (°)	Depth (km)	Horizontal	Vertical
2002/03/20/19/12/6.19	−31.864	−69.49	33.2	4.1	5.6

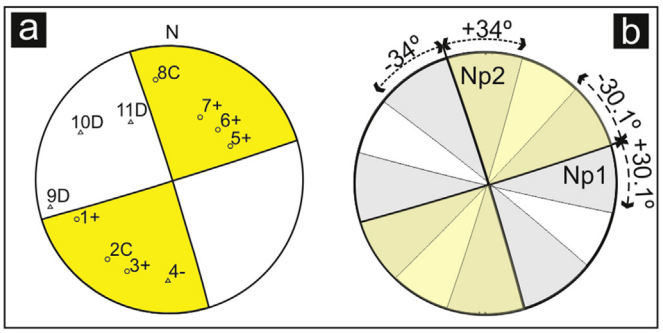

Fig. 10. a) The 11 polarity readings used to calculate the solution are shown as triangles for negatives and circles for positive polarities. We obtained 5 first impulsive movements (indicated with C or D next to the number of the station) and 6 first emergent movements (indicated with the symbol + or - next to the number of the station). There is a reverse polarity (4 station) that corresponds to the low signal-to-noise ratio. Used stations: 1- PACH, 2- PEL, 3- FCH, 4- AREN, 5- LLAN, 6- RINC, 7- HEDI, 8- NEGR, 9- JUAN, 10- LITI, 11- HURT. b) The strike uncertainties of the Np1 and Np2 nodal planes are graphically represented.

318°/69°) at the north of the Precordillera from the study of 33 crustal focal mechanisms. The north and south of the Precordillera have similar tectonic patterns because both have the same direction of maximum compression (WNW-ESE) which result from the partition of the Andean compression along the NNW-SSE-trending structural anisotropies (Cortés et al., 2014).

The north trend of the Precordillera fold-and-thrust belt (Baldis and Chebli, 1969; Ortiz and Zambrano, 1981; Baldis et al., 1982) was traditionally related to orthogonal shortening (Allmendinger et al., 1990; von Gosen, 1992; Zapata and Allmendinger, 1996; Cristallini and Ramos, 2000). On the other hand, regarding the Central Andes Rotation Pattern (Somoza et al., 1996) a dextral transpressional deformation for the Precordillera is proposed by several authors (Japas, 1998; Ré et al., 2001; Siame et al., 2005; Álvarez-Marrón et al., 2006). However, an anti-clockwise rotation induced by several WNW-ESE regional structures was recognized by Japas et al. (2015). Thus, there are four localized NNW-trending oblique belts along the Pampean flat-slab segment between 29°S and 33°S: Valle Fértil (Rossello et al., 1996; Introcaso and Ruiz, 2001), Rodeo-Talacasto (Japas et al., 2011), Mendoza Norte (Ré et al., 2001) or Barreal-Las Peñas (Cortés and Cegarra, 2004; Cortés et al., 2005) and the Río Mendoza-Tupungato (Cortés et al., 2005). The study area is located on the northern sector of the Barreal-Las Peñas belt, where a left-lateral motion is deduced from: 1- local deflections of regional structures (Japas, 1998; Ré et al., 2001) here shown by magnetic anomaly and derived maps; 2 - the preservation of thick neogene deposits in relation to the NW-SE deflection of the main fault in the Sierra de Barreal which is probably associated with quaternary pull apart basins; 3- quaternary folding (Cortés and

Table 3
Focal mechanism solution for the processed earthquake in this work.

Focal Mechanism Solution							
Nodal Plane 1 (°)			Nodal Plane 2 (°)			Uncertainties (°)	
Strike	Dip	Rake	Strike	Dip	Rake	$Strike_{NP1}$	$Strike_{NP2}$
72.9	88.2	−177.6	342.8	87.6	−1.8	30.1	34

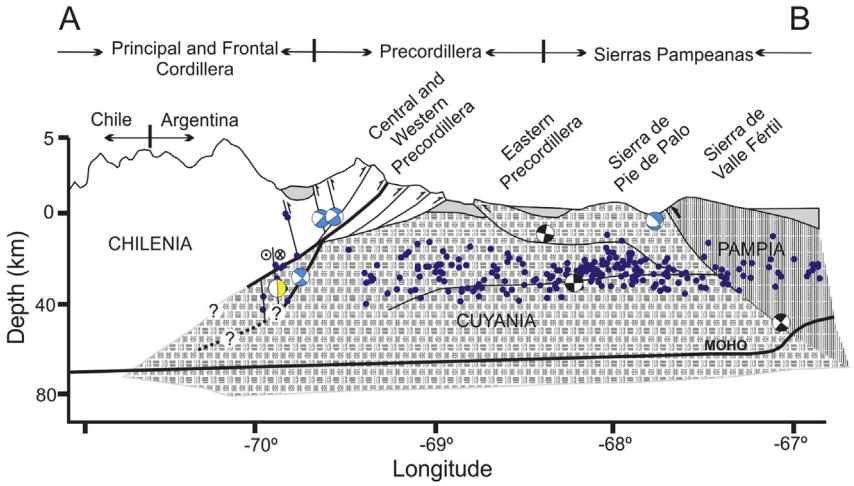

Fig. 11. Results and interpretations beneath the cross-section A–B, (see location Fig. 8). Main geological features are modified from Ramos et al. (2002). Crustal seismicity (blue dots) from Ammirati et al. (2015). Beach balls represent the focal mechanisms in vertical projection along the profile: light blue and white mechanisms from Ammirati et al. (2015); black and white mechanisms from Ramos et al. (2002); with and yellow mechanisms from this work (Table 3). (For interpretation of the references to colour in this figure legend, the reader is referred to the web version of this article.)

Please cite this article in press as: Ariza, J.P., et al., Geological and geophysical evidences of the polyphase structural evolution of the Southern Precordillera (31°42′S-69°24′W), central-western Argentina, Journal of South American Earth Sciences (2017), https://doi.org/10.1016/j.jsames.2017.11.012

Cegarra, 2004; Japas et al., 2011) and kinematic indicators (Japas et al., 2011); 4-crustal seismicity (Ré et al., 2001) and by the seismic event studied in this paper.

5. Conclusions

The Sierra de Barreal, located in the Southern Precordillera of central-western Argentina shows evidences of a polyphase structural evolution. The structures have been developed by three main orogenies that occurred during the Devonian (Chanic), early Permian (San Rafael) and since the Miocene (Andean). From the structural evidences and remote sensing data we interpret a sinistral transpressive geotectonic setting for the Chanic orogeny, where two systems of non-coaxial folds would represent the rotation of the shortening direction (from NW-SE to WSW-ENE) during the deformation. This deformation would have conditioned the subsequent stages of deformation. In this context, the faults and folds developed during the San Rafael orogeny follow the Chanic structural fabric. During the late Cenozoic the Andean orogeny has been locally controlled by inherited anisotropies. This would be confirmed by: the structural style of the Southern Precordillera which in the study area is represented by faulted blocks and west-vergent back-thrusts; neotectonic structures developed in a sinistral transpressive system; the active crustal seismicity associated to NW-SE-trending structures with left-lateral component motion. The similarities between the Chanic transpressive structures and the present tectonic regime of the Barreal-Las Peñas belt would indicate that the sinistral shear zone exerts a strong control over the deformation of the Southern Precordillera.

Acknowledgements

We would like to thank to SEGEMAR for their aero-magnetic flights. This study has been partially financed by research projects CONICET PIP 0072, UBACyT 20020100100862 (both granted to G. Vujovich), PROJOVI-SECITI-UNSJ (granted to J.P. Ariza by Res. 3635-R-2015) and CICITCA - E956 (granted to P. Martinez). We are also grateful to Dr. Christian Creixell Torres and an anonymous reviewer for their very helpful and constructive comments that really improve the early version of the manuscript.

References

Allmendinger, R.W., Figueroa, D., Snyder, D., Beer, J., Mpodozis, C., Isacks, B.L., 1990. Foreland shortening and crustal balancing in the Andes at 30°S latitude. Tectonics 9, 789–809.
Álvarez-Marrón, J., Rodríguez-Fernández, R., Heredia, N., Busquets, P., Colombo, F., Brown, D., 2006. Neogene structures overprinting Palaeozoic thrust systems in the Andean Precordillera at 30° S latitude. J. Geol. Soc., London 163, 949–964.
Álvarez, O., Gimenez, M., Braitenberg, C., Folguera, A., 2012. GOCE satellite derived gravity and gravity gradient corrected for topographic effect in the South Central Andes region. Geophys. J. Int. 190, 941–959.
Ammirati, J.B., Alvarado, P., Beck, S., 2015. A lithospheric velocity model for the flat slab region of Argentina from joint inversion of Rayleigh wave phase veloc-ity dispersion and teleseismic receiver functions. Geophys. J. Int. 202, 224–241.
Amos, A., Marchese, H., 1965. Acerca de una nueva interpretación de la estructura del carbónico en La Ciénaga del Medio. Estancia El Leoncito, sur de Barreal, San Juan. Rev. Asoc. Geol. Argent. 20, 263–270.
Amos, A., Rolleri, E., 1965. El Carbónico marino en el valle Calingasta-Uspallata (San Juan- Mendoza). Bol. Inf. Pet. 368, 50–71.
Ariza, J.P., 2016. Estudios geológicos y geofísicos en la faja ofiolítica de la Precordillera Occidental entre Calingasta y Barreal, San Juan. Evolución geotectónica. PhD Thesis. Universidad Nacional de San Juan, p. 217 (unpublished).
Ariza, J., Martinez, M., Vujovich, G., Sanchez, M., Boedo, F., Pérez, S., 2015. Interpretación estructural de una sección geológica en las nacientes del río San Juan, a partir de datos geológicos y validación geofísica. Rev. Asoc. Geol. Argent. 72, 495–505.
Astini, R., 1992. Tectofacies ordovícicas y evolución de la cuenca eopaleozoica de la Precordillera Argentina. Estud. Geol. 48, 315–327.
Azcuy, C.L., Caminos, R., 1987. Diastrofismo. In: Archangelsky, S. (Ed.), El sistema carbonífero en la República Argentina: Córdoba. Academia Nacional de Ciencias, Argentina, pp. 239–252.
Baldis, B., 1964. Estratigrafía y estructura al sur del arroyo las Cabeceras, estancia El Leoncito. Boletín Informaciones Petroleras 365, 28–33.
Baldis, B., 1975. El Devónico inferior en la Precordillera Central. Parte I: estratigrafía. Rev. Asoc. Geol. Argent. 30, 53–83.
Baldis, B., Chebli, G., 1969. Estructura profunda del área central de la Precordillera sanjuanina. In: 4° Jornadas Geológicas Argentinas, 1. Actas, pp. 47–66.
Baldis, B., Peralta, S., 1999. Silúrico y Devónico de la Precordillera de Cuyo y Bloque de San Rafael. In: Caminos, R. (Ed.), Geología Argentina, Inst. Geol. Rec. Minerales, Anales, vol 29, pp. 215–238.
Baldis, B., Beresi, M., Bordonaro, O., Vaca, A., 1982. Síntesis evolutiva de la Precordillera Argentina. In: 5° Congreso Latinoamericano de Geología, 4. Actas, pp. 399–445.
Baranov, V., 1975. Potential Fields and Their Transformations in Applied Geophysics. Geoexploration Monograph. Series I, 6. Gerbruder Borntraeger, Berlin, Stuttgart, Germany.
Barazangi, M., Isacks, B., 1976. Spatial distribution of earthquakes and subduction of the Nazca plate beneath South America. Geology 4, 686–692.
Blakely, R., 1996. Potential Theory in Gravity and Magnetic Applications. Cambridge University Press., p. 464
Boedo, F.L., Willner, A.P., Vujovich, G.I., Massonne, H.J., 2016. High pressure/low temperature metamorphism in the collision zone between the Chilenia and Cuyania microcontinents (western Precordillera, Argentina). J. S. Am. Earth Sci. 72, 227–240.
Buggisch, W., Gosen, W., von, Henjes-Kunst, F., Krumm, S., 1994. The age of early Paleozoic deformation in metamorphism in the Argentine Precordillera-evidence of K-Ar data. Zentr. Geol. und Paläont. Teil 1, 275–286.
Cheesman, S., MacLeod, I., Hollyer, G., 1998. A new, rapid, automated grid stitching 385 algorithm. Explor. Geophys. 29, 301–305.
Chernicoff, C., Zappettini, E., 2004. Geophysical evidence for terrane boundaries in south-central Argentina. Gondwana Res. 7, 1105–1116.
Cortés, J., 1992. Lavas almohadilladas en el Grupo Ciénaga del Medio, Extremo noroccidental de la Precordillera mendocina. Rev. Asoc. Geol. Argent. 47, 115–117.
Cortés, J.M., Cegarra, M., 2004. Plegamiento cuaternario transpresivo en el piedemonte suroccidental de la Precordillera sanjuanina. In: Cortés, J.M., Rossello, E.A., Dalla Salda, L.H. (Eds.), Avances en Microtectónica. Asociación Geológica Argentina, Buenos Aires Serie D, Publicación Especial, vol. 7, pp. 68–75.
Cortés, J.M., Yamín, M., Pasini, M., 2005. La Precordillera Sur, provincias de San Juan y Mendoza. 16º Congreso Geológico Argentino. Actas 1, 395–402.
Cortés, J.M., Casa, A., Pasini, M., Yamin, M., Terrizzano, C., 2006. Fajas oblicuas de deformación neotectónica en Precordillera y Cordillera Frontal (31° 30′ - 33° 30′ LS): controles paleotectónicos. Rev. Asoc. Geol. Argent. 61, 639–646.
Cortés, J.M., Casa, A., Yamín, M., Pasini, M., Terrizzano, C., 2014. Unidades morfoestructurales, estructuras oblicuas y patrones de distribución de la deformación cuaternaria en la Precordillera de Cuyo (28°-33°S). 19° Congreso Geológico Argentino. Córdoba, S20–S14.
Cristallini, E., Ramos, V., 2000. Thick-skinned and thin-skinned thrusting in the La Ramada fold and thrust belt: crustal evolution of the High Andes of San Juan, Argentina (32°SL). Tectonophysics 317, 205–235.
Cucchi, R.J., 1971. Edades radimétricas y correlación de metamorfitas de la Precordillera, San Juan-Mendoza, República Argentina. Rev. Asoc. Geol. Argent. 26, 503–515.
Dalla Salda, L., Cingolani, C.A., Varela, R., 1992. Early paleozoic belt of the Andes and southwestern South America: result of laurentia-Gondwana collision? Geology 20, 617–620.
Davis, J., Roeske, S., McClelland, W., Snee, L., 1999. Closing the ocean between the Precordillera terrane and Chilenia: early Devonian ophiolite emplacement and deformation in the southwest Precordillera. In: Ramos, V., Keppie, J. (Eds.), Laurentia and Gondwana Connections before Pangea. Geol. Soc. Amer., Spec. Paper, vol 336, pp. 115–138.
Davis, J., Roeske, S., McClelland, W., Kay, S.M., 2000. Mafic and ultramafic crustal fragments of the southwestern Precordillera terrane and their bearing on tectonic models of the early Paleozoic in western Argentina. Geology 28, 171–174.
Dean, W.C., 1958. Frequency analysis for gravity and magnetic interpretation. Geophysics 23, 97–127.
DeMets, C., Gordon, R.G., Argus, D.F., Stein, S., 1990. Current plate motions. Geophys. J. 101, 425–478.
Dobrin, M.B., 1976. Introduction to Geophysical Prospecting. McGraw-hill.
Furlani, R., 2015. Tomografía de sismos locales en el retroarco andino centro-oeste argentino entre 32°S y 33,5°S. Estructura cortical e implicaciones tectónicas. PhD Thesis. Universidad Nacional de San Juan (unpublished).
Furque, G., Cuerda, A., 1979. Precordillera de La Rioja, San Juan y Mendoza. 2° Simposio de Geología Regional Argentina. Acad. Nac. Ciencias Córdoba 1, 237–282.
Gad, S., Kusky, T., 2006. Lithological mapping in the Eastern Desert of Egypt, the Barramiya area, using Landsat thematic mapper (TM). J. Afr. Earth Sci. 44, 196–202.
Gaido, M.F., Cegarra, M., Anselmi, G., Yamín, M., 2008. Hoja Geológica 3169-33, Villa Pituil, 1:100.000, provincia de San Juan. SEGEMAR, 81 pp. (unpublished).
Giambiagi, L., Mescua, J., Folguera, A., Martínez, A., 2010. Estructuras y cinemática de las deformaciones pre-andinas del sector sur de la Precordillera, Mendoza. Rev. Asoc. Geol. Argent. 66, 5–20.
Giambiagi, L., Mescua, J., Bechis, F., Tassara, A., Hoke, G., 2012. Thrust belts of the

Please cite this article in press as: Ariza, J.P., et al., Geological and geophysical evidences of the polyphase structural evolution of the Southern Precordillera (31°42′S-69°24′W), central-western Argentina, Journal of South American Earth Sciences (2017), https://doi.org/10.1016/j.jsames.2017.11.012

Southern Central Andes: along-strike variations in shortening, topography, crustal geometry, and denudation. Geol. Soc. Am. Bull. 124, 1339–1351.
Giambiagi, L., Mescua, J., Heredia, N., Farías, P., García Sansegundo, J., Fernández, C., Stier, S., Pérez, D., Bechis, F., Moreiras, S., Lossada, A., 2014. Reactivation of Paleozoic structures during Cenozoic deformation in the Cordón del Plata and Southern Precordillera ranges Mendoza. Argentina J. Iber. Geol. 40, 309–320.
Hardebeck, J., Shearer, P., 2002. A new method for determining first motion focal mechanisms. Bull. Seismol. Soc. Am. 92, 2264–2276.
Havskov, J., Ottemöller, L., 2010. Routine data processing in earthquake seismology. In: With Sample Data, Exercises and Software. Springer, p. 347.
Heredia, N., Farías, P., García Sansegundo, J., Giambiagi, L., 2012. The basement of the Andean Frontal Cordillera in the Cordón del Plata (Mendoza, Argentina): geodynamic Evolution. Andean Geol. 39, 242–257.
Introcaso, A., Ruiz, F., 2001. Geophysical indicators of Neogene strike-slip faulting in the Desaguadero-Bermejo tectonic lineament (northwestern Argentina). J. S. Am. Earth Sci. 14, 655–663.
Inzana, J., Kusky, T., Higgs, G., Tucker, R., 2003. Supervised classifications of Landsat TM band ratio images and Landsat TM band ratio image with radar for geological interpretations of central Madagascar. J. Afr. Earth Sci. 37, 59–72.
Japas, M.S., 1998. Aporte del análisis de fábrica deformacional al estudio de la faja orogénica andina. Homen. al Dr. Arturo Amos. Rev. Asoc. Geol. Argent. 53, 15.
Japas, M.S., Ré, G.H., Vilas, J.F., Oriolo, S., 2011. Oblique megashear zones in the Precordillera (central Andes, Argentina): the rodeo-Talacasto transpressional belt. In: Deformation, Rheology and Tectonics Conference. Oviedo, Spain.
Japas, M.S., Ré, G.H., Oriolo, S., Vilas, J.F., 2015. Palaeomagnetic data from the Precordillera fold and thrust belt constraining Neogene foreland evolution of the Pampean flat-slab segment (Central Andes, Argentina). In: Pueyo, E.L., Cifelli, F., Sussman, A.J., Oliva-Urcia, B. (Eds.), Palaeomagnetism in Fold and Thrust Belts: New Perspectives. Geological Society, London. Special Publications, 425. http://doi.org/10.1144/SP425.9.
Jordan, T., Isacks, B., Allmendinger, R., Brewer, J., Ando, C., Ramos, V.A., 1983. Andean tectonics related to geometry of subducted plates. Geol. Soc. Am. Bull. 94, 341–361.
Jordan, T.E., Allmendinger, R.W., Damanti, J.F., Drake, R.E., 1993. Chronology of motion in a complete thrust belt: the Precordillera, 30–31°S, Andes Mountains. J. Geol. 101, 137–158.
Leveratto, M.A., 1976. Edad de intrusivos cenozoicos en la Precordillera de San Juan y su implicancia estratigráfica. Rev. Asoc. Geol. Argent. 31, 53–88.
Liener, B.R., Havskov, J., 1995. A computer program for locating earthquakes locally, regionally and globally. Seismol. Res. Lett. 66, 26–36.
Lillesand, T.M., Kiefer, R.W., 1994. Remote Sensing and Image Interpretation, third ed. John Wiley and Sons, Inc., Toronto. p.721.
Llambías, E., Sato, A., 1990. El batolito de Colangüil (29–31°S) Cordillera Frontal de Argentina: estructura y marco tectónico, vol 17. Revista de la Asociación Geológica Argentina, pp. 99–108.
López Gamundí, O.R., 2001. La Formación Majaditas (Carbonífero), flanco occidental de la Precordillera Sanjuanina: litoestratigrafía y facies. Rev. Asoc. Argent. Sedimentol. 8, 57–85.
Martinez, M.P., Gimenez, M.E., 2005. A Preliminary Crustal Geophysic model at 29°18' South latitude based on the observed Bouguer anomaly. In: ISAG 6th International Symposium on Andean Geodynamics. Universitat de Barcelona, Actas, pp. 485–489.
Mesigos, M.G., 1953. El Paleozoico superior de Barreal y su continuación austral "Sierra de Barreal"; (Provincia de San Juan). Rev. Asoc. Geol. Argent. 8, 65–109.
Mpodozis, C., Kay, S.M., 1990. Provincias magmáticas ácidas y evolución tectónica de Gondwana: andes Chilenos (28°-31°S), vol 17. Revista Geológica de Chile, pp. 153–180.
Nabighian, M.N., 1972. The analytic signal of two dimensional magnetic bodies with polygonal cross-sections: its properties and use for automated anomaly interpretation. Geophysics 37, 507–517.
Nabighian, M.N., 1984. Toward a three-dimensional automatic interpretation of potential field data via generalized Hilbert transform: fundamental relations. Geophysics 49, 780–786.
Ortiz, A., Zambrano, J.J., 1981. La provincia geológica Precordillera oriental. In: 8° Congreso Geológico Argentino, 3. Actas, pp. 59–74.
Phillips, J.D., Hansen, R.O., Blakely, R.J., 2007. The use of curvature in potential-field interpretation. Explor. Geophys. 38, 111–119.
Quartino, B., Zardini, R., Amos, A., 1971. Estudio y exploración geológica de la región Barreal- Calingasta, provincia de San Juan, República Argentina. Asociación Geológica Argentina. Monog. N°1, 184.pp.
Ramos, V.A., 1988. Late proterozoic-early paleozoic of South America a collisional history. Episodes 11, 168–174.
Ramos, V.A., 1999a. Plate tectonic setting of the Andean Cordillera. Episodes 22, 183–190.
Ramos, V.A., 1999b. Evolución tectónica de la Argentina. In: Caminos, R. (Ed.), Geología Argentina, Inst. Geol. Rec. Minerales, vol 29, pp. 715–784. Anales.
Ramos, V.A., 2000. Southern central Andes. In: Cordani, U.G., Milani, E.J., Thomaz Fhilo, A., Campos, D.A. (Eds.), Tectonic Evolution of South America, pp. 561–604. Río de Janeiro.
Ramos, V.A., Cristallini, E.O., Pérez, D.J., 2002. The Pampean flat-slab of the Central Andes. J. South Am. Earth Sci. 15, 59–78.
Ramos, V.A., 2009. Anatomy and global context of the Andes: main geologic features and the Andean orogenic cycle. In: Kay, S., Ramos, V., Dickinson, W. (Eds.), Backbone of the Americas: Shallow Subduction, Plateau Uplift, and Ridge and Terrane Collision, vol 204. Geological Society of America Memoir, pp. 31–65.
Ramos, V., Jordan, T., Allmendinger, R., Mpodozis, C., Kay, S., Cortés, J., Palma, M., 1986. Paleozoic terranes of the central Argentine-Chilean Andes. Tectonics 5, 855–888.
Ré, G.H., Japas, M.S., Barredo, S.P., 2001. Análisis de fábrica deformacional (AFD): el concepto fractal cualitativo aplicado a la definición de lineamientos cinemáticos neógenos en el Noroeste Argentino. In: Cortés, J.M., Rossello, E.A., Dalla Salda, L.H. (Eds.), Avances en Microtectónica. Asociación Geológica Argentina, Buenos Aires Serie D: Publicación Especial N°5, pp. 75–82.
Rivas, A.C., 2017. Sismicidad Moderna de la Corteza del norte de la Precordillera. Universidad Nacional de San Juan, p. 118 (unpublished Thesis).
Robinson, D., Bevins, R.E., Rubinstein, N., 2005. Subgreenschist facies metamorphism of metabasites from the Precordillera terrane of western Argentina; constraints on the later stages of accretion onto Gondwana. Eur. J. Mineral 17, 441–452.
Roest, W.R., Verhoef, J., Pilkington, M., 1992. Magnetic interpretation using 3D analytic signal. Geophysics 57, 116–125.
Rossello, E.A., Mozetic, M.E., Cobbold, P.R., Urreiztieta, M., Gapais, D., 1996. El espolón Umango-Maz y la conjugación sintaxial de los lineamientos Tucumán y Valle Fértil (La Rioja, Argentina). 13° Congreso Geológico Argentino y 3° Congreso de Hidrocarburos, pp. 2187–2194. Buenos Aires.
Ruiz, F., Gimenez, M., Martinez, P., Introcaso, A., 2011. Control de calidad de datos aeromagnetométricos. In: La importancia de una adecuada corrección diurna en la interpretación geofísica. 8º Congreso de Exploración y Desarrollo de Hidrocarburos. Actas, pp. 1–11.
Siame, L.L., Bellier, O., Sebrier, M., Araujo, M., 2005. Deformation partitioning in flan subduction setting: case of the Andean foreland of western Argentina (28°S–33°S). Tectonics 24, 1–24.
Somoza, R., Singer, S., Coira, B., 1996. Paleomagnetism of upper Miocene ignimbrites in the Puna: an analysis of vertical-axis rotations in the Central Andes. J. Geophys. Res. 101, 11387–11400.
von Gosen, W., 1992. Structural evolution of the Argentine Precordillera. The río san juan section. J. Struct. Geol. 14, 643–667.
von Gosen, W., 1995. Polyphase structural evolution of the southwestern Argentine Precordillera. J. S. Am. Earth Sci. 8, 377–404.
Willner, A.P., Gerdes, A., Massonne, H.-J., Schmidt, A., Sudo, M., Thomson, S.N., Vujovich, G., 2011. The geodynamics of collision of a microplate (Chilenia) in Devonian times deduced by the pressure-temperature-time evolution within part of a collisional belt (Guarguaraz Complex, W-Argentina). Contrib. Mineral. Petrol. 162, 303–327.
Yamín, M., 2007. Neotectónica del bloque Barreal, margen noroccidental de la Precordillera Sur. PhD Thesis. Universidad de Buenos Aires, p. 281 (unpublished).
Yamín, M., 2009. Falla Barreal (AR-65). En Atlas de Deformaciones Cuaternarias de Los Andes. Proyecto Multinacional Andino: Geociencias para las comunidades andinas (PMA-GCA). Publicación Geológica Multinacional Nº 7, pp. 111–117.
Zapata, T.R., Allmendinger, R.W., 1996. Thrust-front zone of the Precordillera, Argentina; a thick-skinned triangle zone. Am. Assoc. Petrol. Geol. Bull. 80, 359–381.

Please cite this article in press as: Ariza, J.P., et al., Geological and geophysical evidences of the polyphase structural evolution of the Southern Precordillera (31°42′S-69°24′W), central-western Argentina, Journal of South American Earth Sciences (2017), https://doi.org/10.1016/j.jsames.2017.11.012